

Lateral Diffusion, Function, and Expression of the Slow Channel Congenital Myasthenia Syndrome α C418W Nicotinic Receptor Mutation with Changes in Lipid Raft Components*

Received for publication, July 11, 2015, and in revised form, September 1, 2015. Published, JBC Papers in Press, September 9, 2015, DOI 10.1074/jbc.M115.678573

Jessica Oyola-Cintrón^{†1}, Daniel Caballero-Rivera^{‡§2}, Leomar Ballester[§], Carlos A. Baéz-Pagán[§], Hernán L. Martínez[¶], Karla P. Vélez-Arroyo[‡], Orestes Quesada^{||}, and José A. Lasalde-Dominicci^{†§3}

From the Departments of [†]Chemistry, [§]Biology, and ^{||}Physical Sciences, University of Puerto Rico, Rio Piedras Campus, San Juan, Puerto Rico, 00931 and the [¶]California State University Dominguez Hills, Carson, California 90747

Background: α C418W nAChR is the first lipid-exposed mutation identified in a patient that causes slow channel congenital myasthenia syndrome (SCCMS).

Results: The α C418W nAChR is highly immobile and sensitive to lipid raft components.

Conclusion: Cholesterol and CAV-1 modulate the function and dynamics of α C418W nAChRs.

Significance: Understanding the interplay between cholesterol, CAV-1, and nAChRs is crucial for developing potential therapeutic treatments for this disease.

Lipid rafts, specialized membrane microdomains in the plasma membrane rich in cholesterol and sphingolipids, are hot spots for a number of important cellular processes. The novel nicotinic acetylcholine receptor (nAChR) mutation α C418W, the first lipid-exposed mutation identified in a patient that causes slow channel congenital myasthenia syndrome was shown to be cholesterol-sensitive and to accumulate in microdomains rich in the membrane raft marker protein caveolin-1. The objective of this study is to gain insight into the mechanism by which lateral segregation into specialized raft membrane microdomains regulates the activable pool of nAChRs. We performed fluorescent recovery after photobleaching (FRAP), quantitative RT-PCR, and whole cell patch clamp recordings of GFP-encoding *Mus musculus* nAChRs transfected into HEK 293 cells to assess the role of cholesterol and caveolin-1 (CAV-1) in the diffusion, expression, and functionality of the nAChR (WT and α C418W). Our findings support the hypothesis that a cholesterol-sensitive nAChR might reside in specialized membrane microdomains that upon cholesterol depletion become disrupted and release the cholesterol-sensitive nAChRs to the pool of activable receptors. In addition, our results in HEK 293 cells show an interdependence between CAV-1 and α C418W that could confer end plates rich in α C418W nAChRs to a susceptibility to changes in cholesterol levels that could cause adverse drug reactions to cholesterol-

lowering drugs such as statins. The current work suggests that the interplay between cholesterol and CAV-1 provides the molecular basis for modulating the function and dynamics of the cholesterol-sensitive α C418W nAChR.

The nicotinic acetylcholine receptor (nAChR)⁴ is part of the Cys-loop family of ligand-gated ion channels that include: γ -aminobutyric acid, glycine, and 5-hydroxytryptamine. It is an allosteric and integral membrane protein composed of four different subunits arranged pseudo-pentamerically in the stoichiometry of $2\alpha 1:\beta 1:\delta$ or $\epsilon:\gamma$ to form an ion channel. Each subunit contains a large hydrophilic amino-terminal (NH₂) domain that faces the extracellular environment, four transmembrane domains (M1, M2, M3, and M4) made up of 19–25 amino acids, a large cytoplasmic loop between the M3 and M4 domains, and a short extracellular carboxylic terminal (COOH) domain (1–3).

Diseases involving nAChRs can be divided into two broad categories: those in which the structure and function of the nAChR are affected (e.g. congenital myasthenic syndromes, and frontal lobe epilepsy) and those involving a reduction in the number of functional nAChRs (e.g. Alzheimer, Parkinson, and schizophrenia) (4). Because nAChRs are the major type of receptors at the neuromuscular junction they are directly associated to muscle-skeletal diseases like myasthenia gravis and the congenital myasthenia syndrome (CMS) (5). CMS is characterized by a deficiency or kinetic abnormality of the nAChR at the postsynaptic level (6). Mutations that produce CMS are found in all nAChR subunits, including all transmembrane domains and the cytoplasmic loop between transmembrane

* This work was supported, in whole or in part, by National Institutes of Health Grants 1R01GM098343 (to J. A. L. D.) and 1P20GM103642 (to J. R. and J. A. L. D.). The authors declare that they have no conflicts of interest with the contents of this article.

¹ Supported by Research Initiative for Scientific Enhancement (RISE) Program, National Institutes of Health Grant 2 R25 GM061151, and the Puerto Rico Industrial Development Company (PRIDCO).

² Supported by the Research Initiative for Scientific Enhancement (RISE) Program, National Institutes of Health Grant 2 R25 GM061151, the Puerto Rico Industrial Development Company (PRIDCO), and the UPR Golf Tournament Fellowship.

³ To whom correspondence should be addressed: Dept. of Biology, University of Puerto Rico, Rio Piedras Campus, PO Box 23360, San Juan, PR 00931-3360. Tel.: 787-764-0000 (ext: 4887); Fax: 787-753-3852; E-mail: jlasalde@gmail.com.

⁴ The abbreviations used are: nAChR, nicotinic acetylcholine receptor; CAV-1, caveolin-1 protein; CBM, caveoline binding motif; CMS, congenital myasthenia syndrome; D_{app} , approximate diffusion coefficient; FRAP, fluorescent recovery after photobleaching; GFP, green fluorescent protein; M β CD, methyl- β -cyclodextrin; OA, okadaic acid; PI3K, phosphoinositide 3-kinase; PI(4,5)P₂, phosphatidylinositol 4,5-bisphosphate; ROI, region of interest; SCCMS, slow channel congenital myasthenic syndrome.

domains 3 and 4. CMS mutations are classified into two categories: slow channel (prolonged receptor activations) and fast channel (brief receptor activations) syndromes (6). Slow channel congenital myasthenia syndromes (SCCMS) are a group of genetic disorders of neuromuscular transmission characterized by a progressive degeneration of the neuromuscular junction and muscle atrophy leading to fatigability and weakness. The novel SCCMS nAChR mutant α C418W is the first lipid-exposed mutation identified in a patient (7).

Lipid rafts are microdomains of the plasma membrane that contain high concentrations of cholesterol and glycosphingolipids and have been shown to be insoluble in non-ionic detergents. Caveolae, a subset of lipid rafts, are small plasma-membrane invaginations that are rich on the cholesterol-binding protein caveolin-1. The lipid raft hypothesis postulates that some lipid species can associate to form microdomains that can be involved in protein partition, membrane sorting and trafficking, and signaling (8, 9). A fraction of nAChRs occurs in raft domains in mammalian cells, as demonstrated *in vitro* and *in vivo* (10–14).

As a consequence of the Cys to Trp substitution, the lipid-exposed α C418W nAChR mutation introduces a caveolin-binding motif (CBM) into the α M4 transmembrane domain sequence (15). These motifs, which are present in most caveolae-associated proteins, have been shown to favor partitioning of proteins into membrane rafts (16). Previous studies performed by Báez-Pagan *et al.* (15), Santiago *et al.* (17), and Grajales *et al.* (18) have shown that the novel α C418W mutant is sensitive to changes in membrane cholesterol levels and that it preferentially accumulates in CAV-1-positive membrane microdomains. These results suggested that upon cholesterol depletion a significant number of α C418W mutants move from a non-functional to a functional pool of nAChRs and display normal α C418W channel kinetics (15).

A question remains as to the molecular basis for cholesterol regulation of nAChR function and dynamics. Previous studies have postulated two possible mechanisms: 1) that modulation of nAChR function by cholesterol might be associated with lipid bilayer fluidity (19–21) and that 2) cholesterol may act as an “allosteric effector” at some binding sites located within the protein that are distinct from the lipid-protein interface (22–25). Corbing *et al.* (27) mapped the binding sites for cholesterol at the lipid-protein interface of the *Torpedo* nAChR to the α M4, α M1, and γ M4 transmembrane domains. However, Hamouda *et al.* (26) demonstrated that the cholesterol-binding domain fully overlaps the *Torpedo* nAChR lipid-protein interface as cholesterol-binding sites were found in the M4, M3, and M1 transmembrane domains of each subunit. In addition, molecular dynamic simulations have shown that the structure of the nAChR includes internal sites capable of containing cholesterol whose occupation stabilizes protein structure (28). Hence, nAChR-cholesterol interactions are known to regulate the function, dynamics, and number of activable nAChRs; however, the underlying mechanisms are poorly understood (29). Thus, there is a critical need for identifying and gaining insight into the mechanism through which lipid-protein interactions regulate nAChR function and dynamics.

The objective of this study is to gain insight into the mechanism by which lateral segregation into specialized raft membrane microdomains regulates the activable pool of nAChRs. We performed fluorescent recovery after photobleaching (FRAP) experiments and whole cell patch clamp recordings of GFP-encoding *Mus musculus* nAChRs transfected into HEK 293 cells under cholesterol enrichment and depletion conditions to assess the role of cholesterol levels in the diffusion and functionality of the nAChR (WT and α C418W). Lateral diffusion and mobile fraction are modified by either cholesterol enrichment or depletion differently in the α C418W mutant when compared with the WT, further demonstrating the cholesterol-sensitive nature of the α C418W mutant. The low mobile fraction (<14%) displayed by the nAChR provides additional evidence of its trafficking to membrane microdomains. Our findings support the hypothesis that a cholesterol-sensitive nAChR might reside in a specialized membrane microdomain; however, when cholesterol is depleted *in vitro* or *in vivo*, the membrane microdomains disrupt and the cholesterol-sensitive nAChRs are released to the pool of activable receptors. Furthermore, we show a relationship between expression levels of CAV-1 and the α C418W nAChR, a result that has implications on statin treatment of patients expressing this mutation.

Experimental Procedures

Mutagenesis Procedures—*M. musculus* (muscle-type) nAChR subunit cDNAs, subcloned into the cytomegalovirus-based mammalian expression vector pRBG₄, were kindly provided by Anthony Auerbach (SUNY, New York). nAChR ϵ and $-\gamma$ subunit cDNAs, subcloned into the cytomegalovirus-based mammalian expression vector pRK5 and containing an enhanced and “humanized” version of the green fluorescent protein (nGFP) inserted into the Pst1 or Bsu36I site on the M3-M4 loop of the ϵ or γ subunits, respectively, were kindly provided by Veitz Witzemann (Max-Planck-Institut für Medizinische Forschung, Heidelberg, Germany). This humanized version of the enhanced nGFP replaces rare codons for the ones more commonly used in mammalian cells for increased protein expression (30). A previous study using the pRK5- ϵ /GFP and $-\gamma$ /GFP constructs has shown that the introduction of nGFP into the M3-M4 loop of these subunits produces a nAChR indistinguishable from the wild type receptor (31). Desired mutations were engineered with the QuikChangeTM Site-directed Mutagenesis Kit (Stratagene, La Jolla, CA). Oligonucleotide primers were generated with the corresponding mutant codon instead of the wild type (WT) codon at the desired position (Invitrogen). The successful inclusion of mutations was confirmed by DNA sequence analysis performed at the DNA Sequencing Facility in the section of Evolution and Ecology, University of California, Davis, CA.

Cell Culture and Transfection—HEK 293 cells were maintained with Dulbecco’s modified Eagle’s medium (DMEM; Sigma) supplemented with 10% fetal bovine serum (Invitrogen) and 1% of antibiotic antimycotic (Sigma) at 37 °C with 5% CO₂ in the incubator. The ratio of nAChR subunits used for transfection was 2:1:1:1 for α : β : δ : ϵ , where 1 corresponds to 0.7 μ g of cDNA. For FRAP experiments cells were subcultured in a \sim 9.4 cm² borosilicate coverglass chamber (Nalge Nunc Interna-

Lateral Diffusion and Function of α C418W nAChR Mutant

tional, Rochester, NY) at a concentration of 1×10^5 cells/ml the day before transfection. Transfection with wild type (WT) and mutant nAChR subunit cDNAs was performed with FuGENE 6[®] Transfection Reagent (Roche Applied Science, Indianapolis, IN) as instructed by the manufacturer. After the incubation period, cells were washed with PBS once and maintained at 37 °C in DMEM supplemented medium. Cells were used for experiments 3–4 days after transfection. The medium was changed to DMEM without supplements and phenol red just before the experiment.

For electrophysiological experiments, cells were subcultured in a 35-mm culture dish (Corning, Lowell, MA) at a concentration of 1×10^5 cells/ml the day before transfection. Transfection with WT and mutant nAChR subunit cDNAs was performed with FuGENE 6[®] Transfection Reagent (Roche Applied Science) as instructed by the manufacturer. The next day cells were subcultured into 8-mm coverslips and used for experiments 2–3 days after transfection.

For cholesterol content determination, cells were subcultured in 100-mm culture dishes (Nalge Nunc International, Rochester, NY) at a concentration of 1×10^7 cells/ml the day before transfection. Transfection was achieved by the calcium phosphate precipitation method as previously described with some modifications (32). Briefly, the ratio of nAChR subunits used for transfection was 2:1:1:1 for α : β : δ : ϵ , where 1 corresponds to 2 μ g of cDNA per dish. This cDNA mixture was diluted and mixed with 2.5 M CaCl_2 . One volume of this $2 \times \text{Ca}^{2+}$ /DNA solution was mixed with an equal volume of $2 \times$ HEBS solution (274 mM NaCl, 10 mM KCl, 1.4 mM Na_2HPO_4 , 15 mM dextrose, 42 mM HEPES (pH 7.06)) and the $\text{Ca}^{2+} \cdot \text{DNA} \cdot \text{PO}_4^{3-}$ transfection complex was incubated for 20 min at room temperature. For transfections, 1 ml of the $\text{Ca}^{2+} \cdot \text{DNA} \cdot \text{PO}_4^{3-}$ transfection complex was added to the cells and they were incubated for 20 h at 37 °C in DMEM supplemented medium. After the incubation period, cells were washed with PBS once and maintained at 37 °C in DMEM supplemented medium. Cells were used for experiments 3–4 days after transfection.

Electrophysiological Recordings—Whole cell currents were measured in the whole cell configuration of the patch clamp technique using an Axopatch 200B amplifier (Axon Instruments, Inc., Foster City, CA). The bath solution contained 140 mM NaCl, 4 mM KCl, 2 mM CaCl_2 , 1 mM MgCl_2 , 5 mM HEPES, 10 mM glucose (pH 7.4). Pipette solution contained 145 mM KCl, 6 mM MgCl_2 , 7.2 mM K_2HPO_4 , 2.8 mM KH_2PO_4 , 5 mM EDTA (pH 7.4). Pipettes were pulled from thick-wall borosilicate glass with a multistage P-87 Flaming-Brown micropipette puller (Sutter Instruments Co., San Rafael, CA) and fire-polished. Pipette resistances were 2–4 megaohms, and as a reference electrode a 1–2% agar bridge with composition similar to the bath solution was used. Whole cell current traces were electronically filtered at 2 kHz and acquired at 10 kHz. Currents were measured in response to a 300 μ M pulse of acetylcholine (ACh) at a holding potential of -100 mV. Pulse generation, data collection, and analysis were performed with Clampex 10.1 (Axon Instruments, Inc., Foster City, CA).

Membrane Cholesterol Depletion and Enrichment of HEK 293 Cells—Membrane cholesterol depletion or enrichment of HEK 293 cells was accomplished with 30-min incubations in 10 mM methyl- β -cyclodextrin ($\text{M}\beta\text{CD}$) or cholesterol-loaded $\text{M}\beta\text{CD}$, respectively (Sigma). $\text{M}\beta\text{CD}$, a water-soluble cyclic oligosaccharide, has a high affinity for cholesterol and has been extensively used as an effective tool for the transport of cholesterol away from cell surfaces (33). $\text{M}\beta\text{CD}$ incubations selectively remove cholesterol from cell membranes while not affecting membrane integrity when concentrations do not exceed 15 mM (34, 35). After the incubation period, cells were washed with PBS once and the media was changed.

Okadaic Acid Treatment of HEK 293 Cells—HEK 293 cells were incubated with 1 μ M okadaic acid (OA) for 30 min to promote endocytosis of caveolae (Sigma). After the incubation period, cells were washed with PBS once and the media was changed.

PI(4,5) P_2 Levels Modulation—Phosphatidylinositol 4,5-bisphosphate (PI(4,5) P_2) was sequestered by incubating HEK 293 cells overnight in medium with 0.01 M neomycin sulfate (Sigma) or 15 min with 10 μ M wortmannin (Sigma). For PI(4,5) P_2 enrichment, cells were incubated for 15 min with 25 μ M PI(4,5) P_2 (Avanti Polar Lipids, Alabaster, AL).

Cholesterol Determination—800 μ l of each sample were transferred to 50-ml crystal tubes and subjected to the Bligh-Dyer method for the extraction of lipids in solution (36). Briefly, 3.75 ml of 1:2 (v/v) CHCl_3 :MeOH were added to each sample, followed by 1.25 ml of CHCl_3 and 1.25 ml of dH_2O . After each addition, samples were strongly agitated using vortex mixing. The bottom phase (organic phase) of each sample was carefully extracted using a Pasteur pipette. Samples were dried using N_2 (g). Cholesterol content was measured using a commercially available colorimetric assay (Wako Chemicals USA, Richmond, VA).

Fluorescence Recovery After Photobleaching—The two-dimensional translational dynamics of the nAChR on HEK 293 cells were examined by FRAP experiments. FRAP experiments were performed with a Zeiss LSM 510 inverted confocal laser scanning microscope. Temperature, humidity, and CO_2 control during all experiments was achieved using a Tokai Hit (Gendoji-cho, Fujinomiya-shi, Shizuoka, Japan) INUB-ZILCS-F1 motorized stage top incubator with a chamber slide dish attachment and a control unit with an analog gas flow meter. Set point parameters for the chamber were 37 °C with 5% CO_2 . The enhanced and humanized version of the GFP was excited with the 488 nm line of an argon laser with 3–5% transmission. A $\times 100$ 1.4 numeric aperture oil-immersion objective was used for imaging with a 1.03 Airy Units pinhole size. For FRAP measurements, time lapse (512×512 pixels) fluorescent images of a single optical section were taken at 5-ms time intervals before ($n = 3$) and after bleaching with 20 iterations of the 488 nm laser with 100% transmission of a 2.0- μ m circular region of interest (ROI). Data acquisition was performed for 1–2 min afterward. Imaging scans were attenuated to 0.1–1% of the bleaching intensity.

For the quantitative analysis, fluorescent intensities of the bleached region (ROI 1), the reference region inside the same cell (ROI 2), and the extracellular background (ROI 3) were

measured at each time point. Data were corrected for the overall loss in total intensity as a result of the bleach pulse and of the imaging scans (ROI 2), and for extracellular background intensity (ROI 3),

$$F(t) = \frac{ROI(1) - ROI(3)}{ROI(2) - ROI(3)} \quad (\text{Eq. 1})$$

where $F(t)$ is the normalized fluorescence recovery; $ROI(1)$ is the fluorescence intensity of the bleached region at time t ; $ROI(2)$ is the fluorescence intensity of the reference region at time t ; and $ROI(3)$ is the fluorescence intensity at the extracellular background at time t . Fluorescence recovery kinetics was determined by exponential fitting of the corrected data (37–40),

$$f(t) = \sum_{i=1}^m A_i (1 - e^{-Kt}) + B \quad (\text{Eq. 2})$$

where A_i is the amplitude of each component in the sum; t is time; K is the fluorescence decay rate constant related to the half-time fluorescence recovery ($t_{1/2} = \ln(2)/K$); and B is a constant related to the mobile fraction of receptors. In this exponential equation, $m = 1$; hence, exhibiting pseudo-first order kinetics. The mobile fraction of receptors is given by,

$$M_f = \frac{(F_\infty - F_0)}{(F_i - F_0)} \quad (\text{Eq. 3})$$

where M_f is the mobile fraction of receptors; F_∞ is the fluorescence intensity at the end of the FRAP experiment; F_i is the initial fluorescence intensity prior to bleach; and F_0 is the fluorescence intensity immediately after bleach.

GraphPad Prism 4.0 (GraphPad Software Inc., San Diego, CA) and/or Kaleida Graph 4.0 (Synergy Software, Reading, PA) were used to perform nonlinear regression analysis and plotting of the data. The data were fitted by plotting the normalized fluorescence recovery as a function of time. The basic method of analysis for the two-dimensional diffusion of membrane components within a bilayer from FRAP data were developed by Axelrod *et al.* (39). That analysis allows determination of the half-time of fluorescence recovery ($t_{1/2}$), which is used to calculate the lateral diffusion coefficient (D) according to,

$$D = \frac{\gamma\omega^2}{4t_{1/2}} \quad (\text{Eq. 4})$$

where γ is a function of the degree of bleaching with a value of 0.88 for a circular beam (39); and ω is the beam radius (37–39). We obtained $t_{1/2}$ from our fitting ($m = 1$) and used it in conjunction with this equation to find approximate values for the diffusion coefficient of the receptor. This allowed us to make comparisons among the data collected under the different scenarios studied.

Statistical Analysis—Electrophysiological parameters, lateral approximate diffusion coefficients (D_{app}), and mobile fraction (M_f) values were provided as mean \pm S.E. Two-sample comparisons were made using an unpaired t test with Welch's correction. For more than two groups, an analysis of variance with a Dunnett's

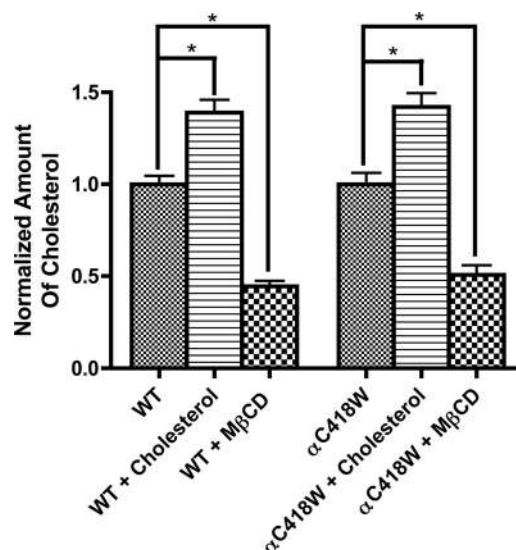


FIGURE 1. Modulation of cholesterol content in HEK 293 cells transfected with the nAChR. Membrane cholesterol levels of HEK 293 cells expressing the WT and α C418W mutant nAChR after cholesterol enrichment or depletion.

post test analysis was performed (GraphPad Software Inc.). A two-tailed p value < 0.05 was considered significant.

Results

Calibration of Cholesterol Levels in HEK 293 Cells and Its Effect on the Localization of Membrane Surface nAChRs—Membrane cholesterol levels of HEK 293 cells expressing the WT and α C418W mutant nAChRs were assessed after cholesterol enrichment or depletion (Fig. 1). Treatment with cholesterol-loaded MβCD caused a statistically significant increase (~40%) in cholesterol levels in HEK 293 cells expressing both the WT and α C418W mutant nAChR, whereas treatment with MβCD produced a statistically significant decrease (~50%) in the cholesterol levels of HEK 293 cells expressing both the WT and α C418W mutant nAChR. These results show that incubation with MβCD and cholesterol-loaded MβCD effectively modulates cholesterol levels in HEK 293 cells.

Lateral Mobility of the WT and the α C418W Mutant nAChR at the Cell Surface of HEK 293 Cells—FRAP of GFP-encoding *M. musculus* nAChRs were performed to examine the lateral mobility of the nAChR at the cell surface of HEK 293 cells (Fig. 2). Cell surface nAChRs exhibited limited mobility as the estimated D_{app} are in the range of 10^{-10} cm²/s (Table 1). The D_{app} of the nAChR at the cell surface of HEK 293 cells corresponds to that of the diffusely distributed nAChR fraction with slow translational mobility reported previously by Axelrod and co-workers (41–43) in rat myotubes and adult rat muscle fibers. Our data show that in HEK 293 cells the mobile fraction of nAChRs is $\leq 14\%$ (Table 1, Fig. 2A), which is consistent with a primarily immobile membrane protein.

The cholesterol-sensitive α C418W mutant nAChR is an α M4 lipid-exposed mutant in which the Trp substitution at position Cys-418 introduces a CBM with the sequence WIIGT-VSVF in *Torpedo californica* and WLIGTLAVF in *M. musculus* (15, 17). A CBM favors partitioning of caveolin-associated proteins into caveolae, a “flask-shaped” subset of lipid raft invagi-

Lateral Diffusion and Function of α C418W nAChR Mutant

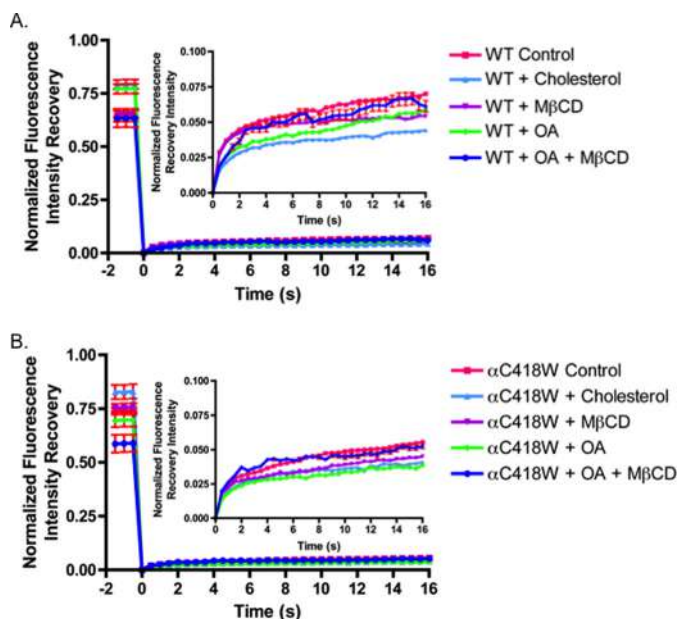


FIGURE 2. Effect of cholesterol enrichment, depletion, and okadaic acid treatment on the lateral diffusion of the *M. musculus* WT nAChR and the novel α C418W mutant. A and B show representative WT and α C418W mutant nAChR FRAP recovery curves, respectively. Recovery curves represent control cells (pink squares), cholesterol-enriched (cholesterol-loaded M β CD; blue triangles), cholesterol-depleted (methyl- β -cyclodextrin, M β CD; purple inverted triangles), okadaic acid (OA; green diamonds), and OA + M β CD (blue circles)-treated cells using a controlled atmosphere (37 °C and 5% CO₂).

TABLE 1

Diffusion parameters and statistical comparison for nAChR subtypes

Error estimates are expressed as the mean \pm S.E. for 8–34 cells.

	Diffusion coefficient	Mobile fraction	$t_{1/2}$	<i>n</i>
	$\times 10^{-10}$ cm ² /s		s	
WT	(5.9 \pm 0.8)	0.14 \pm 0.02	5.9 \pm 0.8	26
WT + cholesterol	(10 \pm 1)	0.061 \pm 0.007 ^a	3.3 \pm 0.4	28
WT + M β CD	(17 \pm 2) ^a	0.086 \pm 0.008 ^a	1.8 \pm 0.3 ^a	23
WT + OA	(4.9 \pm 0.7)	0.088 \pm 0.008 ^a	7.6 \pm 0.9	29
WT + OA + M β CD	(6 \pm 1)	0.12 \pm 0.03	5 \pm 1	8
C418W	(6 \pm 1)	0.086 \pm 0.009 ^b	9 \pm 1 ^b	34
C418W + cholesterol	(9 \pm 2)	0.055 \pm 0.006 ^c	3.8 \pm 0.6 ^d	18
C418W + M β CD	(4.5 \pm 0.6)	0.071 \pm 0.008	7.0 \pm 0.8	24
C418W + OA	(8 \pm 1)	0.063 \pm 0.006	4.7 \pm 0.9 ^d	27
C418W + OA + M β CD	(8 \pm 2)	0.11 \pm 0.07	6 \pm 1	12

^a p < 0.01 compared to WT receptor.

^b p < 0.05 compared to WT receptor.

^c p < 0.05 compared to C418W mutant receptor.

^d p < 0.01 compared to C418W mutant receptor.

nations in the plasma membrane. Consensus CBMs have been established with the following sequences: $\Phi X\Phi XXXX\Phi$ and $\Phi XXXX\Phi XX\Phi$; in which Φ is an aromatic residue (Trp, Phe, or Tyr), and X is any amino acid (16). Variations where one to two apolar amino acids (leucine, isoleucine, or valine) may substitute the aromatic residues have also been reported (44, 45). The mobile fraction of the α C418W mutant nAChR expressed in HEK 293 cells is significantly reduced (0.086 \pm 0.009) when compared with the WT nAChR (0.14 \pm 0.02) under the same controlled conditions (Table 1, Fig. 2, A and B). This reduction in mobility when compared with the WT nAChR could have its origin in the favored aggregation of the α C418W nAChR to form clusters of receptors as previously reported by Báez-Pagan *et al.* (15). In addition, several studies have reported that CAV-1 associated to caveolae has a very low mobile fraction (46). These

results suggest that the α C418W mutant nAChR may be more immobile than the WT nAChR due to a favorable association with CAV-1-positive membrane microdomains that presumably results from the introduction of a CBM.

Effects of Cholesterol Modulation on the α C418W Mutant nAChR—The lateral mobility of nAChRs expressed on HEK 293 cells was examined to assess the role of membrane cholesterol levels on the diffusion of the nAChR (WT and α C418W). Previous studies have shown that the α C418W mutant nAChR expressed in *Xenopus laevis* oocytes is sensitive to changes in membrane cholesterol levels and that it preferentially accumulates in an apparent membrane microdomain in the oocyte membrane (15, 17). The D_{app} of the WT nAChR at the cell surface of HEK 293 cells did not show a statistically significant change upon cholesterol enrichment by cholesterol-loaded M β CD. However, this treatment produced a statistically significant reduction in the mobile fraction of the WT nAChR (Table 1, Fig. 2A). The diffusion coefficient of the WT nAChR upon M β CD treatment increased significantly (\sim 2.9-fold faster fluorescence recovery) as compared with control cells, showing that cholesterol depletion accelerates the motion of the WT nAChR. However, although its diffusion speed may have increased, the mobile fraction of the WT nAChR decreased upon cholesterol depletion when compared with control cells (Table 1, Fig. 2A). This result could be due to an accelerated internalization of a fraction of the cell-surface nAChRs as previously reported by Borroni *et al.* (47).

Membrane cholesterol enrichment by cholesterol-loaded M β CD produced a statistically significant reduction in the mobile fraction of the α C418W mutant nAChR (Table 1, Fig. 2B) without altering the D_{app} as compared with control cells. Cholesterol enrichment of HEK 293 cells produced a statistically significant reduction in macroscopic ACh-induced currents of the α C418W mutant nAChR (Fig. 3B). These results suggest that upon cholesterol enrichment the α C418W mutant nAChRs are internalized into caveolae, where they are trapped in a non-activable state and thus precluded from contributing to the overall macroscopic current. The same cholesterol enrichment did not produce any significant changes in ACh-induced currents of the WT nAChR (Fig. 3A). In contrast, although cholesterol depletion with M β CD does not produce statistically significant changes in the mobile fraction or the D_{app} of the α C418W mutant nAChR, the diffusion coefficient of this mutant in the cholesterol-reduced environment (4.5×10^{-10} cm²/s) is 3.8-fold slower as compared with WT under the same conditions (17×10^{-10} cm²/s). This suggests that this mutant nAChR could still be associated with the scaffolding protein CAV-1 after disruption of lipid rafts (Table 1, Fig. 2, A and B).

Cholesterol depletion in HEK 293 cells expressing the α C418W mutant nAChR produced a remarkable increase (\sim 2-fold) in macroscopic ACh-induced currents (Fig. 3B), suggesting that when lipid rafts are disrupted the α C418W mutant nAChRs are redistributed in the membrane surface where they become activable and contribute to the overall macroscopic current. In contrast, the same cholesterol depletion did not produce any significant changes in ACh-induced currents in the WT nAChR (Fig. 3A). These results demonstrate that in HEK 293 cells the regulation of the α C418W mutation by membrane

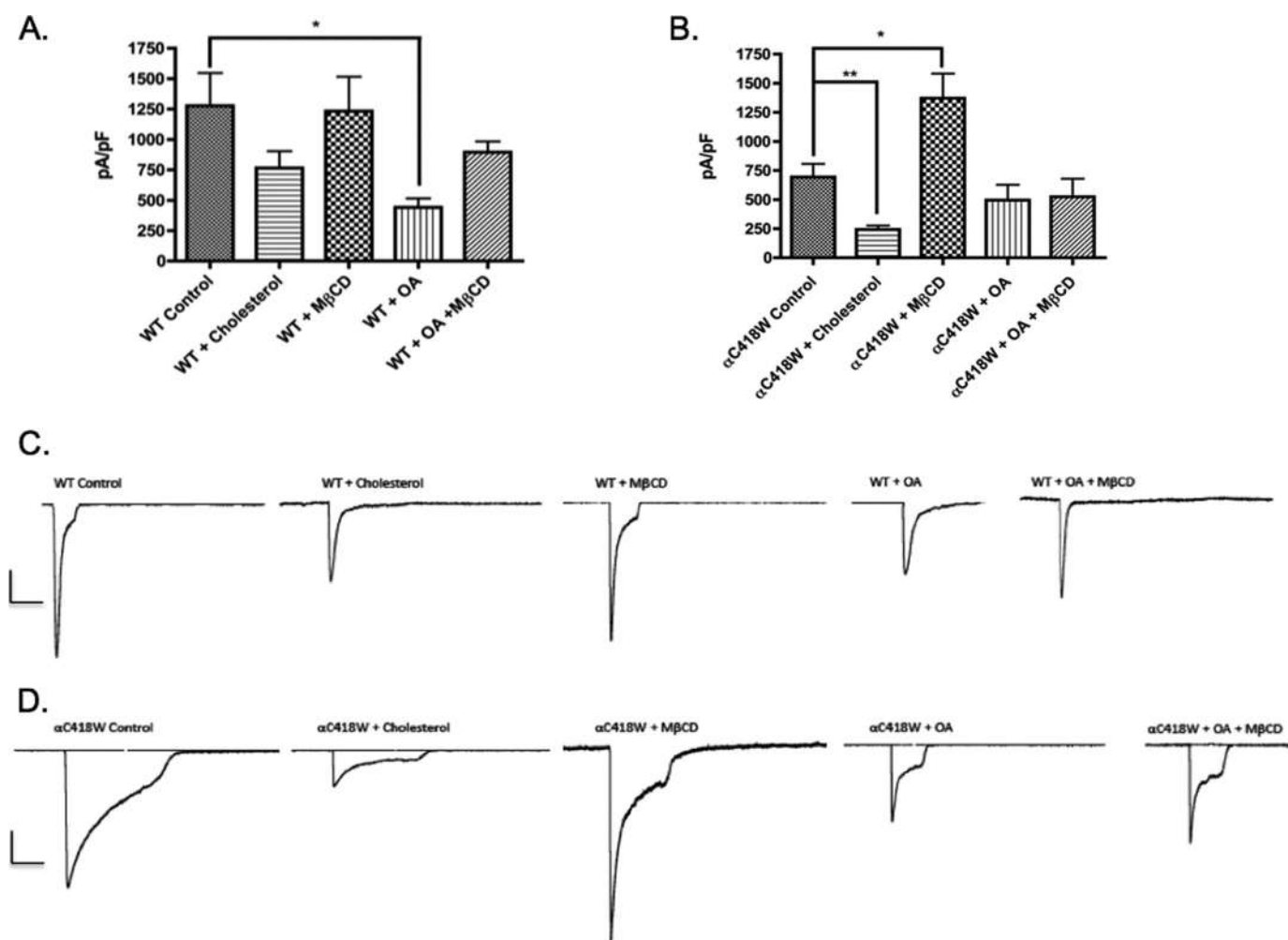


FIGURE 3. Effect of cholesterol enrichment, depletion, and okadaic acid treatment on whole cell currents of the *M. musculus* WT nAChR and the novel α C418W mutant. Whole cell current bar graphs from the (A) WT (control ($n = 8$); + cholesterol ($n = 10$); + M β CD ($n = 8$); + OA ($n = 9$); + OA + M β CD ($n = 8$)) and the (B) α C418W (control ($n = 13$); + cholesterol ($n = 7$); + M β CD ($n = 12$); + OA ($n = 8$); + OA + M β CD ($n = 3$)) nAChR mutant recorded in HEK 293 cells, non-treated or treated with 10 mM M β CD, cholesterol-loaded M β CD, 1 mM OA or OA + M β CD for 30 min. Cholesterol depletion of HEK 293 cells had no effect on the WT whole cell currents while the incubation with OA resulted in a significant reduction in whole cell currents ($p = 0.0176$). However, the same M β CD incubation resulted in a significant increase in the α C418W mutant nAChR whole cell currents, whereas the incubation with cholesterol resulted in a significant decrease in whole cell currents ($p = 0.0119$ and $p = 0.021$, respectively). Neither OA nor OA + M β CD treatments resulted in a significant change in the whole cell currents elicited by the α C418W nAChR. C and D, representative whole cell currents for the WT and mutant α C418W nAChRs corresponding to the mean maximum currents normalized by capacitance depicted on A and B. Scale bar represents 4000 pA on the y axis, 4 s on the x axis.

cholesterol and CAV-1 is consistent with the results described by Báez-Pagan *et al.* (15) in an oocyte expression system.

Association of α C418W Mutant nAChRs with CAV-1 Inside Caveolae Precludes Activation—A previous report by Báez-Pagan *et al.* (15) described how the *Torpedo* α C418W mutant nAChR, expressed in *X. laevis* oocytes, preferentially accumulates in an apparent membrane microdomain in the oocyte surface membrane. This study suggested that a substantial fraction of the α C418W mutant nAChRs is located in a non-activable state while inside cholesterol-dependent CAV-1-positive microdomains, and that lipid raft disruptions due to membrane cholesterol depletion results in the relocation of these mutant nAChRs away from CAV-1-positive microdomains where they could be activated. To determine the potential role of nAChRs located inside CAV-1-positive microdomains, we treated cells with 1 μ M OA, a serine/threonine phosphatase inhibitor known to induce a dramatic endocytosis of caveolae (46, 48). After treatment with OA, the mobile fraction of the WT nAChR at

the cell surface of HEK 293 cells decreased, but no statistically significant differences were observed between the D_{app} of control and OA-treated cells (Table 1, Fig. 2A). Furthermore, whole cell currents of OA-treated cells expressing the WT nAChR were significantly reduced when compared with control cells, but a pre-treatment with OA followed by cholesterol depletion showed no statistically significant differences in whole cell currents (Table 1, Fig. 3A).

In cells transfected with the α C418W mutant nAChR, there were no statistically significant changes in D_{app} and mobile fraction of control and OA-treated cells (Table 1, Fig. 2B). In addition, this treatment did not result in a reduction of α C418W whole cell currents (Fig. 3B). This suggests that although nAChRs are located inside CAV-1-positive microdomains on the cell surface of HEK 293 cells they do not contribute to the macroscopic whole cell current observed upon ACh activation. Moreover, pre-treatment with OA inhibits the increase in macroscopic whole cell current that is produced by

Lateral Diffusion and Function of α C418W nAChR Mutant

TABLE 2

Diffusion parameters and statistical comparison for nAChR subtypes

Error estimates are expressed as the mean \pm S.E. for 19–34 cells.

	Diffusion coefficient	Mobile fraction	$t_{1/2}$	n
	$\times 10^{-10} \text{ cm}^2/\text{s}$		s	
WT	(5.9 \pm 0.8)	0.14 \pm 0.02	5.9 \pm 0.8	26
WT + neomycin	(5.5 \pm 0.9)	0.063 \pm 0.007 ^a	7 \pm 1	24
WT + wortmannin	(11 \pm 2) ^b	0.049 \pm 0.005 ^a	3.9 \pm 0.7	23
WT + PI(4,5)P ₂	(7 \pm 1)	0.066 \pm 0.007 ^a	4.8 \pm 0.7	19
α C418W	(6 \pm 1)	0.086 \pm 0.009 ^b	9 \pm 1 ^b	34
α C418W + neomycin	(10 \pm 1)	0.046 \pm 0.004 ^c	3.1 \pm 0.3 ^c	29
α C418W + wortmannin	(14 \pm 2) ^c	0.039 \pm 0.004 ^c	2.3 \pm 0.3 ^c	24
α C418W + PI(4,5)P ₂	(12 \pm 2) ^c	0.051 \pm 0.004 ^c	3.0 \pm 0.4 ^c	29

^a $p < 0.01$ compared to WT receptor.

^b $p < 0.05$ compared to WT receptor.

^c $p < 0.01$ compared to α C418W mutant receptor.

cholesterol depletion in cells expressing the α C418W nAChR (Fig. 3B). These results show that the α C418W mutant nAChRs that were previously located inside CAV-1-positive microdomains, once relocated across the membrane, can be activated and are responsible, at least in part, for the increase in whole cell currents observed upon cholesterol depletion. The pool of α C418W mutant AChRs segregated to CAV-1-positive microdomains may not be active due to their favorable interaction with CAV-1, a conclusion in agreement with previous studies (15). However, there is no apparent correlation between the nAChR mobile fraction and the increase in whole cell currents observed for the α C418W mutant nAChR.

Effect of PI(4,5)P₂ on the α C418W Mutant nAChR—As stated above, our results show that the α C418W mutant nAChRs located in CAV-1-positive microdomains are at least partially responsible for the increase in whole cell currents observed upon cholesterol depletion. However, the lack of a correlation between the nAChR mobile fraction and whole cell currents observed for the α C418W mutant nAChR suggests that another molecule might also be involved in the regulation of the α C418W mutant nAChR. PI(4,5)P₂ is a key regulatory phospholipid that is abundant inside cholesterol-dependent domains such as lipid rafts (49). This phospholipid has been shown to modulate a wide variety of ion channels including inward-rectifier K⁺ (Kir) (50), mammalian TRP (51), KCNQ family of voltage-gated K⁺ channels (52), amiloride-sensitive epithelial Na⁺ (ENaC) (53, 54), HERG channels (55, 56), CNG channels (57, 58), voltage-gated K⁺ Kv channels (59), and Ca²⁺ release channels such as inositol 1,4,5-trisphosphate receptors and ryanodine receptors (60). However, there is no evidence to date of a direct or indirect interaction between PI(4,5)P₂ and the nAChR. This observation led us to evaluate PI(4,5)P₂ as a potential candidate for a α C418W mutant nAChR modulator.

Neomycin, an antibiotic known to sequester PI(4,5)P₂, produced a statistically significant reduction in the mobile fraction of both the WT and α C418W mutant nAChR (Table 2, Fig. 4, A and B) without altering the D_{app} or whole cell currents (Fig. 5, A and B) as compared with control cells. Treatment with 10 μ M wortmannin, a specific and covalent inhibitor of phosphoinositide 3-kinases (PI3Ks) produced a statistically significant increase in the diffusion coefficient and a statistically significant reduction in mobile fraction for both the WT and α C418W mutant nAChR (Table 2, Fig. 4, A and B) as compared with control cells. In addition, the reduction of PI(4,5)P₂ levels

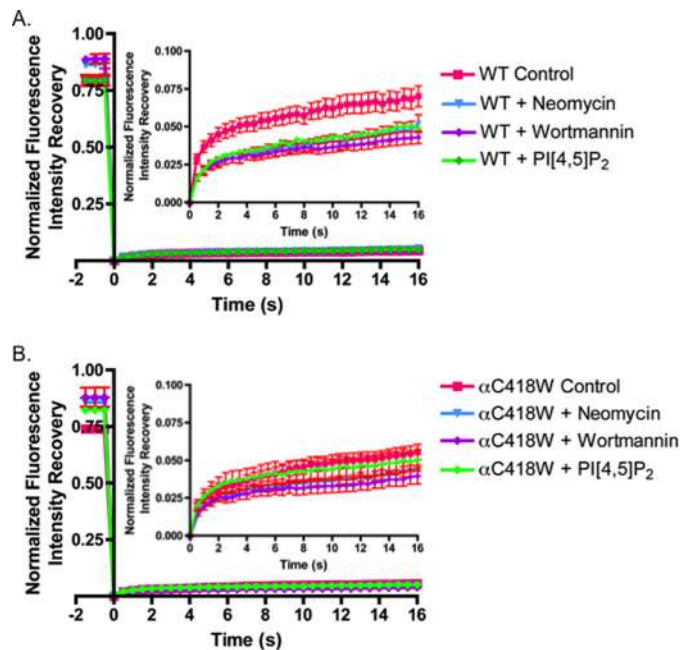


FIGURE 4. Effect of the modulation of PI(4,5)P₂ levels on the lateral diffusion of the *M. musculus* WT and α C418W mutant nAChR. A and B, representative FRAP curves for the WT and α C418W mutant nAChR after incubation with PI(4,5)P₂, the PI(4,5)P₂ sequestering agent neomycin and the PI3K covalent inhibitor wortmannin. Representative recovery curves show WT and α C418W nAChRs (control (pink squares); + neomycin (blue inverted triangles); + wortmannin (purple diamonds); + PI(4,5)P₂ (green diamonds)) treated and untreated cells under a controlled atmosphere (37 °C and 5% CO₂).

caused by treatment of HEK 293 cells with wortmannin produced a statistically significant reduction in whole cell currents for the α C418W mutant nAChR, an effect not observed for the WT nAChR (Fig. 5, A and B). PI(4,5)P₂ enrichment produced a statistically significant reduction in the mobile fraction for the WT nAChR (Table 2, Fig. 4A) without altering the D_{app} or whole cell currents (Fig. 5A) as compared with control cells. The same treatment produced a statistically significant increase in the diffusion coefficient, a statistically significant reduction in mobile fraction (Table 2, Fig. 4B), and no observable changes in whole cell currents (Fig. 5B) for the α C418W mutant nAChR as compared with control cells. It is noteworthy to point out that although their mechanisms of action are different, both neomycin and wortmannin were hypothesized to reduce the whole cell currents for the α C418W mutant nAChR and only the reduction of wortmannin was statistically significant. However, enrichment with PI(4,5)P₂ did not produce the hypothesized increase in whole cell currents. Taken together these results are inconclusive regarding a potential role for PI(4,5)P₂ on the regulation of the α C418W mutant nAChR.

Discussion

The mobile fraction of nAChRs expressed in HEK 293 cells was determined to be $\leq 14\%$ (Table 1, Fig. 2A), which is consistent with a primarily immobile membrane protein. This immobility might be due to receptor clustering mediated by intermolecular receptor-receptor associations, interactions with non-receptor scaffolding or cytoskeleton proteins, and/or protein-lipid interactions (61). A recent study combined FRAP and confocal fluorescence correlation spectroscopy to examine the

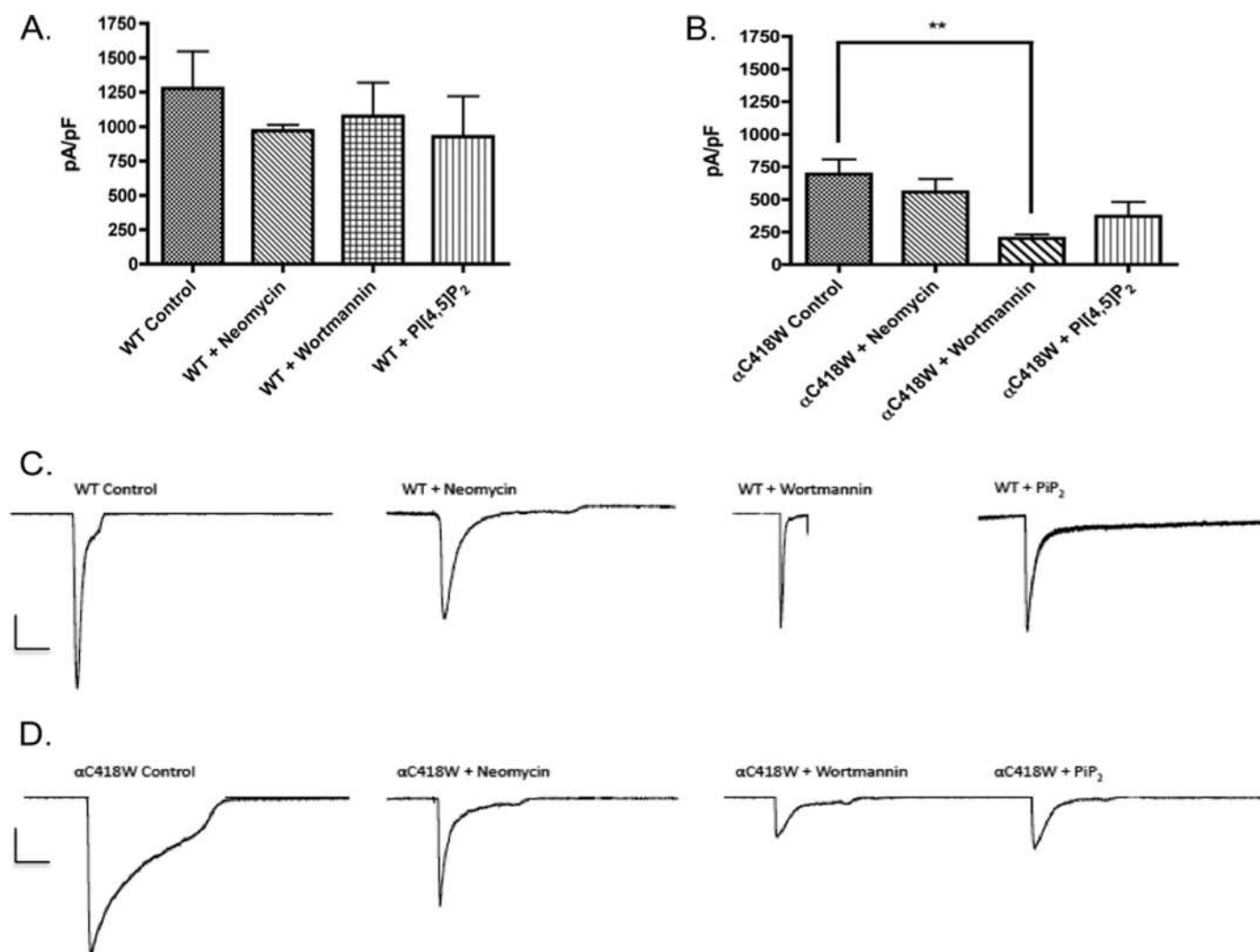


FIGURE 5. Effect of the modulation of PI(4,5)P₂ levels on whole cell currents of the *M. musculus* WT and α C418W mutant nAChR. A and B, whole cell current bar graphs from the WT (control ($n = 9$); + neomycin ($n = 5$); + wortmannin ($n = 5$); + PI(4,5)P₂ ($n = 6$)) and the α C418W (control ($n = 13$); + neomycin ($n = 14$); + wortmannin ($n = 8$); + PI(4,5)P₂ ($n = 7$)) nAChR mutant recorded in HEK 293 cells. PI(4,5)P₂ sequestering with neomycin had no statistically significant effect on whole cell currents elicited by ACh for the WT and α C418W nAChRs. However, inhibition of PI3K with wortmannin resulted in a decrease in whole cell currents elicited by ACh for the α C418W nAChR ($p = 0.0010$). Addition of PI(4,5)P₂ to transfected cells showed no statistically significant effects on ACh elicited currents for neither the WT nor the α C418W mutant nAChR. C and D, representative whole cell currents for WT and mutant α C418W nAChRs corresponding to the mean maximum currents normalized by capacitance depicted on A and B. Scale bar represents 4000 pA on the y axis, 4 s on the x axis.

mobility of the AChR and its dependence on cholesterol levels at the cell surface of a mammalian CHO-K1/A5 cell line (62). This minimalist mammalian expression model produces heterologous adult murine muscle-type acetylcholine receptors, and lacks rapsyn and other receptor-anchoring proteins. Depletion of membrane cholesterol by m β CD strongly affected the mobility of the AChR at the plasma membrane, reducing the mobile fraction by 35% in cholesterol-depleted cells, whereas cholesterol enrichment did not affect receptor mobility at the cell surface (62). These results were confirmed by scanning fluorescence correlation spectroscopy experiments that showed that the diffusion coefficient of the AChR was \sim 30% lower upon cholesterol depletion. That study suggested that membrane cholesterol modulates AChR mobility at the plasma membrane through a cholesterol-dependent mechanism sensitive to cortical actin (62).

The α C418W nAChR from *T. californica* has been previously shown to be sensitive to changes in membrane cholesterol

levels and that a substantial fraction of these mutant nAChRs accumulates in CAV-1-positive membrane microdomains in the oocyte surface membrane, where they are trapped in a non-activable state (15). FRAP experiments performed on HEK 293 cells showed that the mobile fraction of the α C418W mutant nAChR was significantly reduced when compared with the WT nAChR. These results correlate with the phenotype associated to the α C418W nAChR in SCCMS in which a 30% reduction in the number of α C418W nAChRs in HEK cells is reported when compared with the WT nAChR (7). In addition, several studies have reported that CAV-1 associated to caveolae has a very low mobile fraction (46). Based on the introduction of a CBM upon tryptophan substitution at position Cys-418, we propose that the α C418W mutant nAChR is less mobile than the WT nAChR due to favorable association with CAV-1-positive membrane microdomains.

Báez-Pagan *et al.* (15) demonstrated that the increase in macroscopic peak currents observed upon cholesterol depletion

Lateral Diffusion and Function of α C418W nAChR Mutant

was not due to changes in α C418W nAChR kinetics or conductance, but rather an increase in the number of receptors in the oocyte surface membrane as a consequence of cholesterol depletion. To determine the mechanism that regulates the activable pool of nAChRs in a mammalian expression system we modulated cholesterol levels in the surface membrane of HEK 293 cells. Membrane cholesterol enrichment by cholesterol-loaded M β CD produced a statistically significant reduction in both the mobile fraction and macroscopic ACh-induced currents of the α C418W mutant nAChR. This result was expected as it has been previously demonstrated that cholesterol enrichment affects nAChR trafficking through the endocytic pathway, decreasing cell-surface expression by promoting internalization of nAChRs (63). However, cholesterol depletion in HEK 293 cells expressing the α C418W mutant nAChR produced a remarkable increase (~2-fold) in macroscopic ACh-induced currents, suggesting that when lipid rafts are disrupted the α C418W mutant nAChRs are redistributed in the membrane surface where they become activable and contribute to the overall macroscopic current. These results demonstrate that in HEK 293 cells the regulation of the α C418W mutation by membrane cholesterol and CAV-1 is consistent with the results described by Báez-Pagan *et al.* (15) when the mutant is expressed in *X. laevis* oocytes.

Treatment with OA did not result in a reduction of α C418W whole cell currents (Fig. 3B) and a pre-treatment with OA before cholesterol depletion inhibits the increase in macroscopic whole cell current that is produced by cholesterol depletion in cells expressing the α C418W nAChR (Fig. 3B). These results suggest that α C418W mutant nAChRs expressed in CAV-1-positive domains are trapped in a non-activable state and thus precluded from contributing to the overall macroscopic current observed upon ACh activation due to their favorable interaction with CAV-1. Taken together these results suggest there is no apparent correlation between the nAChR mobile fraction and whole cell currents for either the WT or α C418W mutant nAChR under cholesterol-depleted conditions.

Fluorescence recovery curves provide information on two parameters: the diffusion coefficient provides a measure of the kinetics of translational mobility, whereas the mobile fraction reports on the proportion of fluorescent molecules in the membrane surface that are able to laterally diffuse back into the bleached area over time. Recently, Báez-Pagan (15) showed an increase in the number of α C418W mutant nAChRs available to be activated in the membrane surface upon cholesterol depletion and how that effect translated into higher whole cell currents. However, as is the case in the current study a higher number of receptors in the membrane surface does not necessarily translate to a higher mobile fraction. Previous studies have shown that the mobility of raft- and non-raft resident proteins decreases when cholesterol is depleted from the membrane surface (64, 65). Other studies have postulated that restricted diffusion of membrane proteins upon cholesterol depletion stems from the formation of solid-like clusters in the membrane (66, 67). Lowering membrane cholesterol levels with M β CD alters membrane viscosity and has been shown to hinder membrane protein diffusion (68). In addition, it has been proposed that changes in cholesterol levels affect the

mechanical properties of plasma membrane through the underlying cytoskeleton (69). Fernandes *et al.* (70) showed that nAChR mobility is subtype specific as cholesterol depletion with M β CD increased the mobility of neuronal α 7 nAChRs but not that of α 3 nAChRs in the central nervous system synapses.

Recently, a transgenic mouse model expressing the SCCMS α C418W mutant nAChR was used to demonstrate *in vivo* that the single-nucleotide polymorphism rs137852808 (α C418W) was sensitive to changes in membrane cholesterol levels (18), a result in agreement with what we have observed in HEK 293 cells. Furthermore, this mutation produced in mice a myopathy-like picture after statin treatment similar to statin-induced adverse drug reactions. Mice expressing this allele showed a remarkable contamination of end plates with CAV-1 and developed signs of neuromuscular degeneration upon statin treatment as the percentage of CAV-1-positive neuromuscular junctions was significantly reduced. The reduction in the percentage of end plates displaying co-localization of α C418W and CAV-1 in statin-treated neuromuscular junctions suggested that these end plates are sensitive to cholesterol concentration. Our results in HEK 293 cells supports the notion of an interdependence between CAV-1 and the α C418W nAChR that is observed in the neuromuscular junction, and that confers the α C418W nAChR end plate a susceptibility to changes in cholesterol levels that can lead to adverse drug reactions due to modifications in end plate plasticity.

PI(4,5)P₂ is an abundant phospholipid inside lipid rafts that has been linked to the regulation of a wide diversity of ion channels. This led us to hypothesize that it could be a potential candidate for a α C418W mutant nAChR modulator. The reduction of PI(4,5)P₂ levels caused by treatment of HEK 293 cells with wortmannin, a PI3K inhibitor, produced a statistically significant reduction in whole cell currents for the α C418W mutant nAChR, an effect not observed for the WT nAChR. However, this reduction in whole cell currents was not observed when using the PI(4,5)P₂ sequestering agent neomycin. In addition, enrichment with PI(4,5)P₂ did not produce the hypothesized increase in whole cell currents. Additional studies will be needed to clarify the role, if any, that PI(4,5)P₂ might play on the regulation of the α C418W mutant nAChR.

Author Contributions—J. O. C., D. C. R., and J. A. L. designed the study. J. O. C., D. C. R., C. A. B., and J. A. L. wrote the paper. J. O. C., K. P. V., and D. C. R. designed the plasmids, prepared DNAs and RNAs, and cultivated and treated cells. D. C. R. designed siRNAs and PCR primers. J. O. C. and D. C. R. performed FRAP and gene knock-down experiments. L. B., D. C. R., and J. O. C. performed whole cell electrophysiology experiments. O. Q. performed cholesterol content determinations. All authors analyzed the results and approved the final version of the manuscript.

Acknowledgments—We thank the UPR Confocal Imaging Facility and the UPR Cell Culture Facility. In addition, we thank Anthony Auerbach for the *M. musculus* (muscle-type) AChR subunit cDNAs and Veitz Witzemann for the *M. musculus* ϵ -GFP and γ -GFP AChR subunit cDNAs.

References

- Karlin, A., and Akabas, M. H. (1995) Toward a structural basis for the function of nicotinic acetylcholine receptors and their cousins. *Neuron* **15**, 1231–1244
- Hucho, F., Tsetlin, V. I., and Machold, J. (1996) The emerging three-dimensional structure of a receptor: the nicotinic acetylcholine receptor. *Eur. J. Biochem.* **239**, 539–557
- Corringer, P. J., Le Novère, N., and Changeux, J. P. (2000) Nicotinic receptors at the amino acid level. *Annu. Rev. Pharmacol. Toxicol.* **40**, 431–458
- Léna, C., and Changeux, J. P. (1997) Pathological mutations of nicotinic receptors and nicotine-based therapies for brain disorders. *Curr. Opin Neurobiol.* **7**, 674–682
- Lindstrom, J. (1997) Nicotinic acetylcholine receptors in health and disease. *Mol. Neurobiol.* **15**, 193–222
- Engel, A. G., Ohno, K., and Sine, S. M. (2002) The spectrum of congenital myasthenic syndromes. *Mol. Neurobiol.* **26**, 347–367
- Shen, X. M., Deymeier, F., Sine, S. M., and Engel, A. G. (2006) Slow-channel mutation in acetylcholine receptor α M4 domain and its efficient knock-down. *Ann. Neurol.* **60**, 128–136
- Simons, K., and Ikonen, E. (1997) Functional rafts in cell membranes. *Nature* **387**, 569–572
- Simons, K., and van Meer, G. (1988) Lipid sorting in epithelial cells. *Biochemistry* **27**, 6197–6202
- Brusés, J. L., Chauvet, N., and Rutishauser, U. (2001) Membrane lipid rafts are necessary for the maintenance of the α 7 nicotinic acetylcholine receptor in somatic spines of ciliary neurons. *J. Neurosci.* **21**, 504–512
- Campagna, J. A., and Fallon, J. (2006) Lipid rafts are involved in C95 (4,8) agrin fragment-induced acetylcholine receptor clustering. *Neuroscience* **138**, 123–132
- Stetzkowski-Marden, F., Gaus, K., Recouvreur, M., Cartaud, A., and Cartaud, J. (2006) Agrin elicits membrane lipid condensation at sites of acetylcholine receptor clusters in C2C12 myotubes. *J. Lipid Res.* **47**, 2121–2133
- Stetzkowski-Marden, F., Recouvreur, M., Camus, G., Cartaud, A., Marchand, S., and Cartaud, J. (2006) Rafts are required for acetylcholine receptor clustering. *J. Mol. Neurosci.* **30**, 37–38
- Willmann, R., Pun, S., Stallmach, L., Sadasivam, G., Santos, A. F., Caroni, P., and Fuhrer, C. (2006) Cholesterol and lipid microdomains stabilize the postsynapse at the neuromuscular junction. *EMBO J.* **25**, 4050–4060
- Báez-Pagán, C. A., Martínez-Ortiz, Y., Otero-Cruz, J. D., Salgado-Villanueva, I. K., Velázquez, G., Ortiz-Acevedo, A., Quesada, O., Silva, W. I., and Lasalde-Dominicci, J. A. (2008) Potential role of caveolin-1-positive domains in the regulation of the acetylcholine receptor's activatable pool: implications in the pathogenesis of a novel congenital myasthenic syndrome. *Channels* **2**, 180–190
- Okamoto, T., Schlegel, A., Scherer, P. E., and Lisanti, M. P. (1998) Caveolins, a family of scaffolding proteins for organizing "preassembled signaling complexes" at the plasma membrane. *J. Biol. Chem.* **273**, 5419–5422
- Santiago, J., Guzmán, G. R., Rojas, L. V., Martí, R., Asmar-Rovira, G. A., Santana, L. F., McNamee, M., and Lasalde-Dominicci, J. A. (2001) Probing the effects of membrane cholesterol in the *Torpedo californica* acetylcholine receptor and the novel lipid-exposed mutation α C418W in *Xenopus* oocytes. *J. Biol. Chem.* **276**, 46523–46532
- Grajales-Reyes, G. E., Báez-Pagán, C. A., Zhu, H., Grajales-Reyes, J. G., Delgado-Vélez, M., García-Beltrán, W. F., Luciano, C. A., Quesada, O., Ramírez, R., Gómez, C. M., and Lasalde-Dominicci, J. A. (2013) Transgenic mouse model reveals an unsuspected role of the acetylcholine receptor in statin-induced neuromuscular adverse drug reactions. *Pharmacogenomics J.* **13**, 362–368
- Baenziger, J. E., Morris, M. L., Darsaut, T. E., and Ryan, S. E. (2000) Effect of membrane lipid composition on the conformational equilibria of the nicotinic acetylcholine receptor. *J. Biol. Chem.* **275**, 777–784
- Sunshine, C., and McNamee, M. G. (1994) Lipid modulation of nicotinic acetylcholine receptor function: the role of membrane lipid composition and fluidity. *Biochim. Biophys. Acta* **1191**, 59–64
- Fong, T. M., and McNamee, M. G. (1986) Correlation between acetylcholine receptor function and structural properties of membranes. *Biochemistry* **25**, 830–840
- Antollini, S. S., and Barrantes, F. J. (1998) Disclosure of discrete sites for phospholipid and sterols at the protein-lipid interface in native acetylcholine receptor-rich membrane. *Biochemistry* **37**, 16653–16662
- Fernandez-Ballester, G., Castresana, J., Fernandez, A. M., Arrondo, J. L., Ferragut, J. A., and Gonzalez-Ros, J. M. (1994) Role of cholesterol as a structural and functional effector of the nicotinic acetylcholine receptor. *Biochem. Soc. Trans.* **22**, 776–780
- Narayanaswami, V., and McNamee, M. G. (1993) Protein-lipid interactions and *Torpedo californica* nicotinic acetylcholine receptor function: 2. Membrane fluidity and ligand-mediated alteration in the accessibility of γ subunit cysteine residues to cholesterol. *Biochemistry* **32**, 12420–12427
- Jones, O. T., and McNamee, M. G. (1988) Annular and nonannular binding sites for cholesterol associated with the nicotinic acetylcholine receptor. *Biochemistry* **27**, 2364–2374
- Hamouda, A. K., Sanghvi, M., Sauls, D., Machu, T. K., and Blanton, M. P. (2006) Assessing the lipid requirements of the *Torpedo californica* nicotinic acetylcholine receptor. *Biochemistry* **45**, 4327–4337
- Corbin, J., Wang, H. H., and Blanton, M. P. (1998) Identifying the cholesterol binding domain in the nicotinic acetylcholine receptor with [¹²⁵I]-azido-cholesterol. *Biochim. Biophys. Acta* **1414**, 65–74
- Brannigan, G., Héning, J., Law, R., Eckenhoff, R., and Klein, M. L. (2008) Embedded cholesterol in the nicotinic acetylcholine receptor. *Proc. Natl. Acad. Sci. U.S.A.* **105**, 14418–14423
- Barrantes, F. J. (2004) Structural basis for lipid modulation of nicotinic acetylcholine receptor function. *Brain Res. Brain Res. Rev.* **47**, 71–95
- Zolotukhin, S., Potter, M., Hauswirth, W. W., Guy, J., and Muzyczka, N. (1996) A "humanized" green fluorescent protein cDNA adapted for high-level expression in mammalian cells. *J. Virol.* **70**, 4646–4654
- Gensler, S., Sander, A., Korngreen, A., Traina, G., Giese, G., and Witzemann, V. (2001) Assembly and clustering of acetylcholine receptors containing GFP-tagged ϵ or γ subunits: selective targeting to the neuromuscular junction *in vivo*. *Eur. J. Biochem.* **268**, 2209–2217
- Jordan, M., Schallhorn, A., and Wurm, F. M. (1996) Transfecting mammalian cells: optimization of critical parameters affecting calcium-phosphate precipitate formation. *Nucleic Acids Res.* **24**, 596–601
- Christian, A. E., Haynes, M. P., Phillips, M. C., and Rothblat, G. H. (1997) Use of cyclodextrins for manipulating cellular cholesterol content. *J. Lipid Res.* **38**, 2264–2272
- Anderson, T. G., Tan, A., Ganz, P., and Seelig, J. (2004) Calorimetric measurement of phospholipid interaction with methyl- β -cyclodextrin. *Biochemistry* **43**, 2251–2261
- Niu, S. L., Mitchell, D. C., and Litman, B. J. (2002) Manipulation of cholesterol levels in rod disk membranes by methyl- β -cyclodextrin: effects on receptor activation. *J. Biol. Chem.* **277**, 20139–20145
- Bligh, E. G., and Dyer, W. J. (1959) A rapid method of total lipid extraction and purification. *Can. J. Biochem. Physiol.* **37**, 911–917
- Klonis, N., Rug, M., Harper, I., Wickham, M., Cowman, A., and Tilley, L. (2002) Fluorescence photobleaching analysis for the study of cellular dynamics. *Eur. Biophys. J.* **31**, 36–51
- Yguerabide, J., Schmidt, J. A., and Yguerabide, E. E. (1982) Lateral mobility in membranes as detected by fluorescence recovery after photobleaching. *Biophys. J.* **40**, 69–75
- Axelrod, D., Koppel, D. E., Schlessinger, J., Elson, E., and Webb, W. W. (1976) Mobility measurement by analysis of fluorescence photobleaching recovery kinetics. *Biophys. J.* **16**, 1055–1069
- Marty, S., Schroeder, M., Baker, K. W., Mazzanti, G., and Marangoni, A. G. (2009) Small-molecule diffusion through polycrystalline triglyceride networks quantified using fluorescence recovery after photobleaching. *Langmuir* **25**, 8780–8785
- Axelrod, D., Ravdin, P., Koppel, D. E., Schlessinger, J., Webb, W. W., Elson, E. L., and Podleski, T. R. (1976) Lateral motion of fluorescently labeled acetylcholine receptors in membranes of developing muscle fibers. *Proc. Natl. Acad. Sci. U.S.A.* **73**, 4594–4598
- Stya, M., and Axelrod, D. (1983) Mobility and detergent extractability of acetylcholine receptors on cultured rat myotubes: a correlation. *J. Cell Biol.* **97**, 48–51
- Stya, M., and Axelrod, D. (1984) Mobility of extrajunctional acetylcholine

Lateral Diffusion and Function of α 418W nAChR Mutant

- receptors on denervated adult muscle fibers. *J. Neurosci.* **4**, 70–74
44. Couet, J., Li, S., Okamoto, T., Ikezu, T., and Lisanti, M. P. (1997) Identification of peptide and protein ligands for the caveolin-scaffolding domain: implications for the interaction of caveolin with caveolae-associated proteins. *J. Biol. Chem.* **272**, 6525–6533
45. Carman, C. V., Lisanti, M. P., and Benovic, J. L. (1999) Regulation of G protein-coupled receptor kinases by caveolin. *J. Biol. Chem.* **274**, 8858–8864
46. Thomsen, P., Roepstorff, K., Stahlhut, M., and van Deurs, B. (2002) Caveolae are highly immobile plasma membrane microdomains, which are not involved in constitutive endocytic trafficking. *Mol. Biol. Cell* **13**, 238–250
47. Borroni, V., Baier, C. J., Lang, T., Bonini, I., White, M. M., Garbus, I., and Barrantes, F. J. (2007) Cholesterol depletion activates rapid internalization of submicron-sized acetylcholine receptor domains at the cell membrane. *Mol. Membr Biol.* **24**, 1–15
48. Parton, R. G., Joggerst, B., and Simons, K. (1994) Regulated internalization of caveolae. *J. Cell Biol.* **127**, 1199–1215
49. Huang, C. L. (2007) Complex roles of PIP2 in the regulation of ion channels and transporters. *Am. J. Physiol. Renal Physiol.* **293**, F1761–1765
50. Hilgemann, D. W., and Ball, R. (1996) Regulation of cardiac Na^+ , Ca^{2+} exchange and KATP potassium channels by PIP2. *Science* **273**, 956–959
51. Rohacs, T. (2007) Regulation of TRP channels by PIP_2 . *Pflugers Arch.* **453**, 753–762
52. Delmas, P., and Brown, D. A. (2005) Pathways modulating neural KCNQ/M (Kv7) potassium channels. *Nat. Rev. Neurosci.* **6**, 850–862
53. Ma, H. P., Saxena, S., and Warnock, D. G. (2002) Anionic phospholipids regulate native and expressed epithelial sodium channel (ENaC). *J. Biol. Chem.* **277**, 7641–7644
54. Pochynyuk, O., Staruschenko, A., Tong, Q., Medina, J., and Stockand, J. D. (2005) Identification of a functional phosphatidylinositol 3,4,5-trisphosphate binding site in the epithelial Na^+ channel. *J. Biol. Chem.* **280**, 37565–37571
55. Bian, J., Cui, J., and McDonald, T. V. (2001) HERG K^+ channel activity is regulated by changes in phosphatidylinositol 4,5-bisphosphate. *Circ. Res.* **89**, 1168–1176
56. Bian, J. S., Kagan, A., and McDonald, T. V. (2004) Molecular analysis of PIP2 regulation of HERG and IKr. *Am. J. Physiol. Heart Circ. Physiol.* **287**, H2154–2163
57. He, F., Mao, M., and Wensel, T. G. (2004) Enhancement of phototransduction G protein-effector interactions by phosphoinositides. *J. Biol. Chem.* **279**, 8986–8990
58. Womack, K. B., Gordon, S. E., He, F., Wensel, T. G., Lu, C. C., and Hilgemann, D. W. (2000) Do phosphatidylinositides modulate vertebrate phototransduction? *J. Neurosci.* **20**, 2792–2799
59. Oliver, D., Lien, C. C., Soom, M., Baukrowitz, T., Jonas, P., and Fakler, B. (2004) Functional conversion between A-type and delayed rectifier K^+ channels by membrane lipids. *Science* **304**, 265–270
60. Suh, B. C., and Hille, B. (2008) PIP2 is a necessary cofactor for ion channel function: how and why? *Annu. Rev. Biophys.* **37**, 175–195
61. Barrantes, F. J. (2014) Cell-surface translational dynamics of nicotinic acetylcholine receptors. *Front. Synaptic Neurosci.* **6**, 25
62. Baier, C. J., Gallegos, C. E., Levi, V., and Barrantes, F. J. (2010) Cholesterol modulation of nicotinic acetylcholine receptor surface mobility. *Eur. Biophys. J.* **39**, 213–227
63. St. John, P. A. (2009) Cellular trafficking of nicotinic acetylcholine receptors. *Acta Pharmacol. Sin.* **30**, 656–662
64. Kenworthy, A. K., Nichols, B. J., Remmert, C. L., Hendrix, G. M., Kumar, M., Zimmerberg, J., and Lippincott-Schwartz, J. (2004) Dynamics of putative raft-associated proteins at the cell surface. *J. Cell Biol.* **165**, 735–746
65. O'Connell, K. M., and Tamkun, M. M. (2005) Targeting of voltage-gated potassium channel isoforms to distinct cell surface microdomains. *J. Cell Sci.* **118**, 2155–2166
66. Nishimura, S. Y., Vrljic, M., Klein, L. O., McConnell, H. M., and Moerner, W. E. (2006) Cholesterol depletion induces solid-like regions in the plasma membrane. *Biophys. J.* **90**, 927–938
67. Vrljic, M., Nishimura, S. Y., Moerner, W. E., and McConnell, H. M. (2005) Cholesterol depletion suppresses the translational diffusion of class II major histocompatibility complex proteins in the plasma membrane. *Biophys. J.* **88**, 334–347
68. Shvartsman, D. E., Gutman, O., Tietz, A., and Henis, Y. I. (2006) Cyclodextrins but not compactin inhibit the lateral diffusion of membrane proteins independent of cholesterol. *Traffic* **7**, 917–926
69. Sun, M., Northup, N., Marga, F., Huber, T., Byfield, F. J., Levitan, I., and Forgacs, G. (2007) The effect of cellular cholesterol on membrane-cytoskeleton adhesion. *J. Cell Sci.* **120**, 2223–2231
70. Fernandes, C. C., Berg, D. K., and Gómez-Varela, D. (2010) Lateral mobility of nicotinic acetylcholine receptors on neurons is determined by receptor composition, local domain, and cell type. *J. Neurosci.* **30**, 8841–8851

Lateral Diffusion, Function, and Expression of the Slow Channel Congenital Myasthenia Syndrome α C418W Nicotinic Receptor Mutation with Changes in Lipid Raft Components

Jessica Oyola-Cintrón, Daniel Caballero-Rivera, Leomar Ballester, Carlos A. Baéz-Pagán, Hernán L. Martínez, Karla P. Vélez-Arroyo, Orestes Quesada and José A. Lasalde-Dominicci

J. Biol. Chem. 2015, 290:26790-26800.

doi: 10.1074/jbc.M115.678573 originally published online September 9, 2015

Access the most updated version of this article at doi: [10.1074/jbc.M115.678573](https://doi.org/10.1074/jbc.M115.678573)

Alerts:

- [When this article is cited](#)
- [When a correction for this article is posted](#)

[Click here](#) to choose from all of JBC's e-mail alerts

This article cites 70 references, 31 of which can be accessed free at <http://www.jbc.org/content/290/44/26790.full.html#ref-list-1>